Pergamon

Journal of Structural Geology, Vol. 19, No. 1, pp. 15 to 27, 1997

0191-8141/97 $17.00+0.00

PII: S0191-8141(96)00075-2

Origin and incremental evolution of brittle/ductile shear zones in granitic rocks: natural examples from the southern Abitibi Belt, Canada

GHISLAIN TOURIGNY*

Ministère des Ressources Naturelles du Québec, Service géologique du Nord-Ouest, 400 blvd Lamaque, Val d'Or, Québec J9P 3L4, Canada

and

ALAIN TREMBLAY

INRS-Géoressources, Centre géoscientifique de Québec, 2535 blvd Laurier, C.P. 7500, Sainte-Foy, Québec G1V 4C7, Canada

(*Received* 14 *November* 1995; *accepted in revised form* 30 *August* 1996)

Abstract—Metre-scale shear zones developed in the Mooshla granitic pluton exhibit a plethora of internal meso- and microstructures revealing their mode of nucleation, growth and termination. The subvertical E–W brittle/ductile shear zones are developed in the most isotropic part of the intrusion and consist of phyllonites characterized by mylonitic fabrics and well-developed down-dip mineral lineations. They are exposed on a single, large and flat outcrop perpendicular to the mineral lineation.

These brittle/ductile shear zones are in close spatial association with a fracture system along which they have nucleated and propagated. Joints, fractures and brittle faults contain abundant evidence of ductilely deformed and recrystallized minerals suggesting that they underwent ductile shearing after their formation. The deformation was accompanied by the influx of a metasomatic fluid which altered original Fe–Mg-bearing minerals and plagioclase into quartz, epidote, chlorite, sericite and carbonate that precipitated in dilatant fractures and narrow breccia zones. We recognize two different types of lateral terminations: (i) shear zones that terminate into joints and fractures that are parallel or oblique to the shear direction, and (ii) curved segments of shear zones that connected with neoformed splay fractures at high angle to the shear direction. In the latter case, sharp bending and severe perturbation of the shear zone orientation occur at the shear zone termination where ductile shearing is transfered into an adjacent shear zone via dilatational fractures. This demonstrates that shear zones tended to grow towards each other and coalesce to form a well-developed anastomosing network.

We propose that narrow dilatational fractures and joints acted as paleo-weakness planes along which fluid–rock interaction and resulting reaction-softening occurred. The deformation scenario involves episodic fluid drawn into dilatant sites responsible for cyclic fluid pressure fluctuation in the system. Dilatancy-related fracturing and reaction-softening lead to deformation under brittle-to-plastic conditions and to shear strain localization.

INTRODUCTION

Shear zones are localized areas of large shear strain accumulation relative to surrounding rocks (Ramsay and Graham, 1970). Past and recent studies on ductile and brittle/ductile shear zones have focused on understanding their dynamic evolution and mode of development (Mitra, 1978, 1992; Ramsay and Allison, 1979; Bell and Hammond, 1984; Simpson, 1985; Losh, 1989; Gibson, 1990; FitzGerald and Stünitz, 1993, among others). Small-scale ductile and brittle/ductile shear zones (cm- to metre-scale) are of particular interest in studies concerning the nucleation and termination of ductile deformation because one can look at: (1) Deformation mechanisms and processes involved in strain localization; (2) The lateral and dip-slip strain propagation; and (3) The geometrical evolution of progressive deformation.

For isotropic rocks such as granitoids, Burg and Laurent (1978) recognized two types of ductile shear zones: continuous and discontinuous. The first type is characterized by a continuous and progressive increase of the shear strain from the shear zone boundary (which is more or less well defined) to the center of the shear zone where the most highly strained rocks are localized. The second type shows discontinuous increase of the shear strain. It is characterized by sharp boundaries between highly strained central areas and unstrained or relatively less deformed adjacent domains (Burg and Laurent, 1978; Vauchez, 1987). The shear zone boundaries are commonly well-defined, subparallel to the mylonitic foliation and look like faults.

For granitic rocks, Ramsay and Allison (1979) described the formation of high-temperature (amphibolite-grade) continuous ductile shear zones that are mainly characterized by a progressive decrease in the angle between the foliation plane (assumed to be parallel to the X–Y plane of finite deformation) and the shear zone boundaries. In high-grade metamorphic settings, the nucleation of continuous shear zones is believed to be

*Present address: Corporation Lithos, 1137 3[e]rue, C.P. 876, Val d'Or, Québec, J9P 4P8 Canada.

independent of pre-existing fractures and is commonly attributed to shear instabilities induced both by the internal characteristics of the protolith (e.g. grain-size and compositional heterogeneities) and by deformation conditions (e.g. stress state, strain rate, etc. see Ramsay, 1980; White *et al.*, 1980; Takagi, 1989 and Hanmer and Passchier, 1991 for reviews). Discontinuous ductile shear zones also exist in high-temperature environments, for example, Vauchez (1987) described intimately associated continuous and discontinuous ductile shear zones and stressed the existence of a genetic link between these two end-members.

Low-temperature (sub-greenschist- and greenschist-grade) ductile and brittle/ductile shear zones in granitic rocks have been described by Mitra (1978, 1992), Williams and Dixon (1982), Segall and Pollard (1983), Segall and Simpson (1986), Simpson (1983, 1985), O'Hara (1988), Losh (1989), Gibson (1990), Evans (1990), FitzGerald and Stünitz (1993) and Stünitz and FitzGerald (1993) among others. Most of these studies stressed the importance of fluids for the promotion of brittle fracturing and chemical softening that lead to strain localization and the development of ductile deformation zones (Mitra, 1978; Williams and Dixon, 1982; O'Hara, 1988; Losh, 1989; Gibson, 1990; FitzGerald and Stünitz, 1993). Segall and Pollard (1983) and Segall and Simpson (1986) have suggested that low-temperature, brittle/ductile shear zones frequently nucleate along dilatant fractures.

Natural examples of shear zone terminations have been described by Ramsay and Allison (1979), Simpson (1983), Segall and Pollard (1983) and McGrath and Davison (1995) with theoretical reviews by Coward (1976), Ingles (1986) and Bürgmann and Pollard (1994). A ductile shear zone is a planar zone of finite dimension and should be thus characterized both by dip-slip and lateral tip terminations (i.e. exposed in sections respectively parallel (*XZ*) and perpendicular (*YZ*) to the shear direction for a dip-slip fault; see Fig. 1). Most well-described natural examples of ductile shear zone terminations are for the lateral tips of strike-slip faults (Ramsay and Allison, 1979; Simpson, 1983; Segall and Pollard, 1983). Lateral propagation features of dip-slip brittle/ductile shear zones are presently poorly documented except for regionally-developed fault systems (Boyer and Elliott, 1982; Coward and Potts, 1983; Newman and Mitra, 1993).

This contribution describes the mode of nucleation and growth of greenschist-grade natural shear zones developed in the Mooshla pluton of the southern Abitibi greenstone belt. South-dipping, normal-sense shear zones are described from a subhorizontal outcrop, perpendicular to the inferred transport direction (Fig. 1). Microscopic and mesoscopic structures preserved both in the pluton and in crosscutting shear zones record early increments of brittle deformation that were coeval with fluid infiltration, hydration of plagioclase and Fe–Mg minerals, thereby causing subsequent softening and ductile strain localization. A bulk regime of brittle failure both preceded and succeeded ductile shearing, so that deformation conditions have been mainly controlled by varying fluid/rock ratios through time.

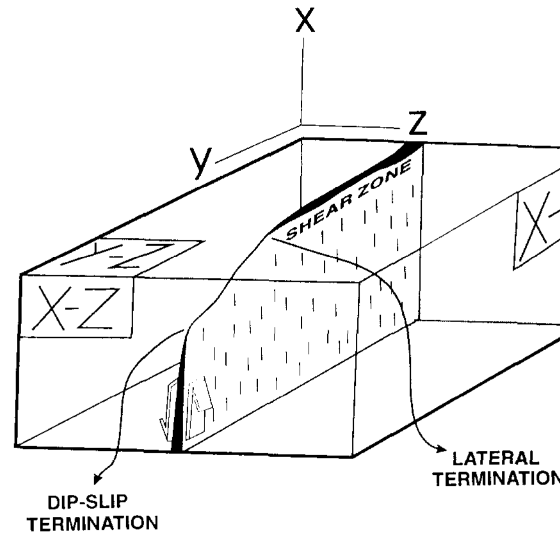

Fig. 1. Block diagram illustrating propagation features of a typical dip-slip shear zones. Dip-slip terminations are those that can be observed parallel to the tectonic transport direction (on *XZ* planes) whereas lateral terminations can be observed along planes perpendicular to both the transport direction and the mylonitic foliation (on *YZ* planes).

REGIONAL SETTING

The studied shear zones are exposed in a single large outcrop of the Archean Mooshla pluton in the Bousquet gold district of Québec (Fig. 2). This mining district lies in the southeastern part of the Abitibi greenstone belt in the Superior Province of the Canadian Shield.

Supracrustal rocks of the area consist of polydeformed Archean volcano–sedimentary assemblages of mafic to felsic volcanic and volcaniclastic rocks flanked by clastic sedimentary rock units (Stone, 1990) (Fig. 2). The volcanic and sedimentary rocks strike EW to NW–SE, dip steeply towards the south and display a moderate to strong bedding-parallel foliation with predominantly down-dip stretching and mineral lineations. Regional structures and fabrics are attributed to N–S compression during the Late Archean Kenoran orogeny (Ludden *et al.*, 1986). Regional metamorphism attained the greenschist–amphibolite facies transition and was followed by retrograde metamorphism to lower greenschist facies conditions (Dimroth *et al.*, 1983).

EW-trending subvertical faults, typically localized along major lithological contacts, are the dominant structural features of the area (Fig. 2). One of these is the Cadillac–Larder Lake fault that separates the Abitibi greenstone belt to the north from the Pontiac Subprovince to the south. The Cadillac–Larder Lake fault and its related structures are characterized by complex

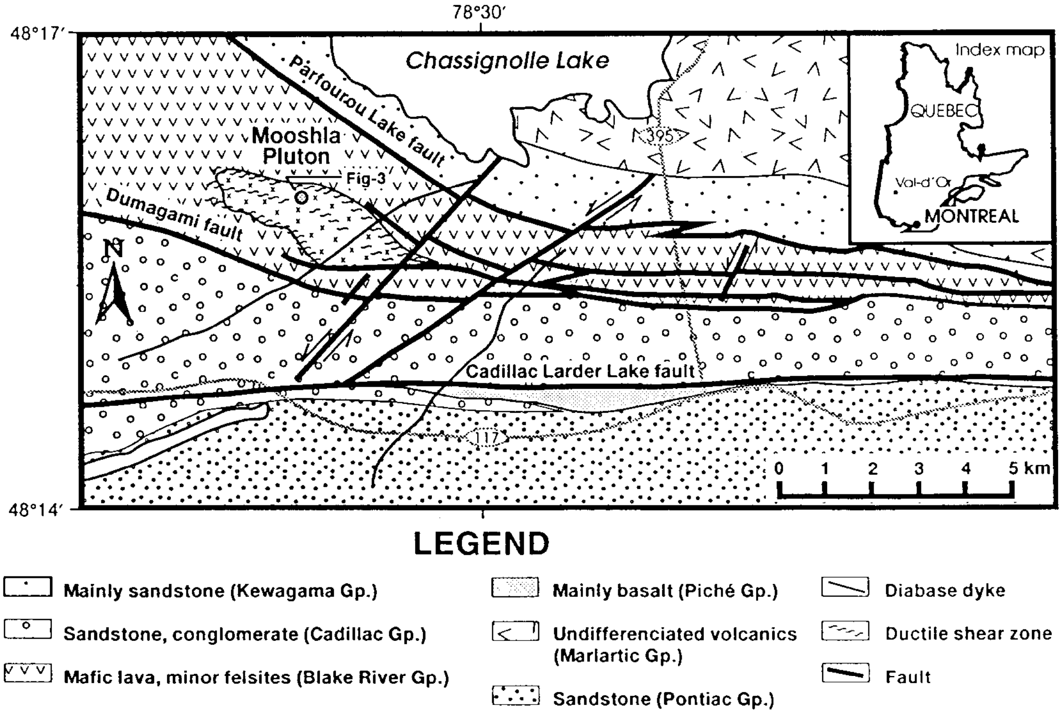

Fig. 2. Geological map of the Bousquet gold district. The area is located 45 km west of Val d'Or (see inset map).

structures involving high-angle reverse faulting and/or dextral transpression (Robert, 1989; Tourigny, 1991; Tourigny and Chartrand, 1994). Youngest tectonic structures of the area are represented by NE-trending, sinistral strike-slip faults that have only minor influence on the internal geometry of surrounding volcanic and sedimentary rocks (Fig. 2).

The Mooshla pluton crosscuts the Blake River Group (Fig. 2), a bimodal volcanic sequence which has been dated at ca 2703–2701 Ma (Corfu *et al.*, 1989, Mortensen, 1993). The pluton is a shear-bounded elliptical body that ranges in composition from gabbro to tonalite and trondhjemite. On the basis of its petrological trend and geochemical signatures, which are similar to those of the Blake River volcanics, the Mooshla pluton is interpreted as a syn-volcanic intrusion (Gaudreau, 1986; Langshur, 1991).

BRITTLE/DUCTILE SHEAR ZONES OF THE MOOSHLA PLUTON

The studied area is located about 4 km to the north of the Cadillac–Larder Lake fault zone, in the northern half of the Mooshla pluton (Fig. 2). The outcrop is dominated by a medium- to coarse-grained tonalite that is characterized by a relict equigranular igneous texture (Fig. 3). The tonalite is composed of approximately 50–60 % zoned subhedral to euhedral plagioclase, 15–25% euhedral quartz, 10–15% ferromagnesian minerals, and by apatite, titanite, zircon and pyrite as accessory minerals. Plagioclase grains are 1–5 mm in diameter and locally show Albite and Carlsbad twinning. Zoned plagioclase crystals vary from An_{15-25} (cores) to An_{3-8} (rims) (Langshur, 1991). Quartz (1–4 mm) exhibit lobate grain boundaries and show undulatory extinction. Primary micrographic textures of quartz and albite are locally well-preserved. Plagioclase is variably replaced and contains a variety of patchy minerals such as epidote, sericite and calcite along many healed and sealed microfractures. Ferromagnesian minerals consist mostly of 5 mm-long needles of hornblende (actinolite) and biotite replaced by chlorite, quartz and sulphides.

The tonalite is crosscut by NNW–SSE to N–S-trending subvertical aplite dykes. These cm-thick aplitic dykes are fine-grained and almost entirely composed of twinned plagioclase, euhedral quartz and accessory zircon with interstitial epidote, muscovite and chlorite. U–Pb zircon dating of the aplite dyke that crosscuts the tonalite in Fig. 3 yielded a crystallization age of 2702 ± 4 Ma (Tremblay *et al.*, 1995).

Mesoscopic structural features

At the studied locality (Figs 2 & 3), the tonalite is crosscut by shear zones that are characterized by bands of intense ductile shearing associated with a pervasive sericitic and pyritic alteration. Wall-rock alteration envelopes are symmetrically developed on both sides of shear zones, and form 1–5 cm-wide border zones. The shear zones include a major EW-trending set and a minor NW- to NNW-trending set (Fig. 3). Shear zones of the EW-trending set dip moderately to steeply towards the south, whereas those of the NW- to NNW-trending set are steeply inclined toward the southwest (Fig. 3). The minor set of shear zones shows the same mineralogy,

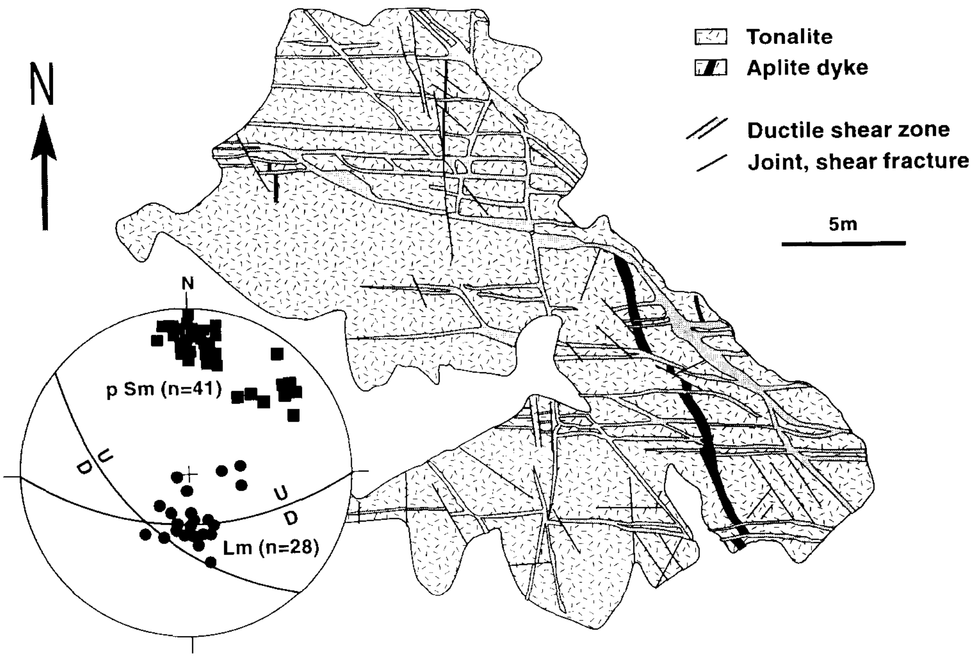

Fig. 3. Detailed geological map of the studied outcrop of the Mooshla pluton. Note the mutually cross-cutting relationships between the different sets of brittle/ductile shear zones and between the E–W trending shear zones and the aplite dyke. In the lower left, lower-hemisphere equal-area stereographic plot of poles to the mylonitic foliation (squares) of the E–W and NW–SE trending sets of ductile/brittle shear zones, and of mineral lineations (dots).

alteration features and kinematic characteristics as the EW-trending shear zones, and both sets are mutually cross-cutting and interpreted to be contemporeneous.

The thickness of shear zones ranges from less than 1 cm to more than 50 cm, and they extend from 10 metres to approximately 50 metres along strike (Fig. 3). Both continuous and discontinuous shear zones, as described by Burg and Laurent (1978), are found (Fig. 4a & b). Continuous shear zones have diffuse gradational contacts with the nearly undeformed tonalite within less than 5 cm. The contacts are marked by 0.5–2 mm-size, quartz and altered plagioclase porphyroclasts set in a fine-grained matrix of chlorite–epidote–sericite–quartz. A pervasive mylonitic fabric is defined by aligned phyllosilicates and by incipient porphyroclast tails and quartz ribbons. Discontinuous shear zones are in sharp contact with the fractured but relatively undeformed tonalite. Shear zone boundaries usually coincide with discrete, very fine-grained and well-foliated phyllosilicate-rich slip planes composed of chlorite–sericite–quartz with variable amounts of epidote and ferruginous insoluble material. Plagioclase porphyroclasts are commonly absent. Shear zones characterized by sharp boundaries on one side and gradual boundaries on the opposite side are also observed, but discontinuous shear zones predominate over continuous shear zones. Within the shear zones, the tonalitic protolith is transformed into a quartz–mica phyllonite characterized by a compositional layering comprising chlorite–sericite–epidote-rich layers and quartz–sericite-rich layers. In hand specimen, the phyllosilicate-rich layers give the rock a dark green color, and the layering imparts a well-defined mylonitic appearance. The sub-greenschist to greenschist facies mineral assemblages in the phyllonite indicate a temperature of approximately 250–400°C during deformation. The mylonitic foliation, S_m, is defined by alternating chlorite–sericite–epidote and quartz-rich layers whereas the mineral lineation is marked by chlorite-rich strips that plunge moderately to steeply towards the south (Fig. 3).

On subhorizontal surfaces approximately perpendicular to the mineral lineation, EW- and NW-trending shear zones form an anastomosing pattern (Figs 3 & 4c) with intervening lenses of less deformed tonalite. Within the EW-trending shear zones, S_m locally defines a sigmoidal fabric that indicates an apparent dextral or sinistral sense of shear (Fig. 4a). In vertical sections parallel to the mineral lineation, S_m strikes parallel to shear zone boundaries but is consistently less steeply dipping towards the south (Fig. 4d). On such sections, S_m describes sigmoidal forms and coexists with *C*/*S* fabrics, both of which indicate that the sense of shearing is top towards the south (Fig. 4d). In the central part of many shear zones, there are millimetre-wide zones of intense shearing marked by well-developed *C*/*S* fabrics where the *C*-planes are parallel to the shear zone boundaries, and commonly correspond to quartz- and sulphide-rich slip surfaces. In vertical sections, NNW-trending shear zones display structural and kinematic features similar to the EW-trending shear zones. Aplite dykes intruding the tonalite can be observed to crosscut the shear zones (Fig. 4e), or to be crosscut by the major set of shear zones (Fig. 4f), thus indicating that their emplacement is broadly coeval with ductile shearing at 2702 ± 4 Ma (Tremblay *et al.*, 1995).

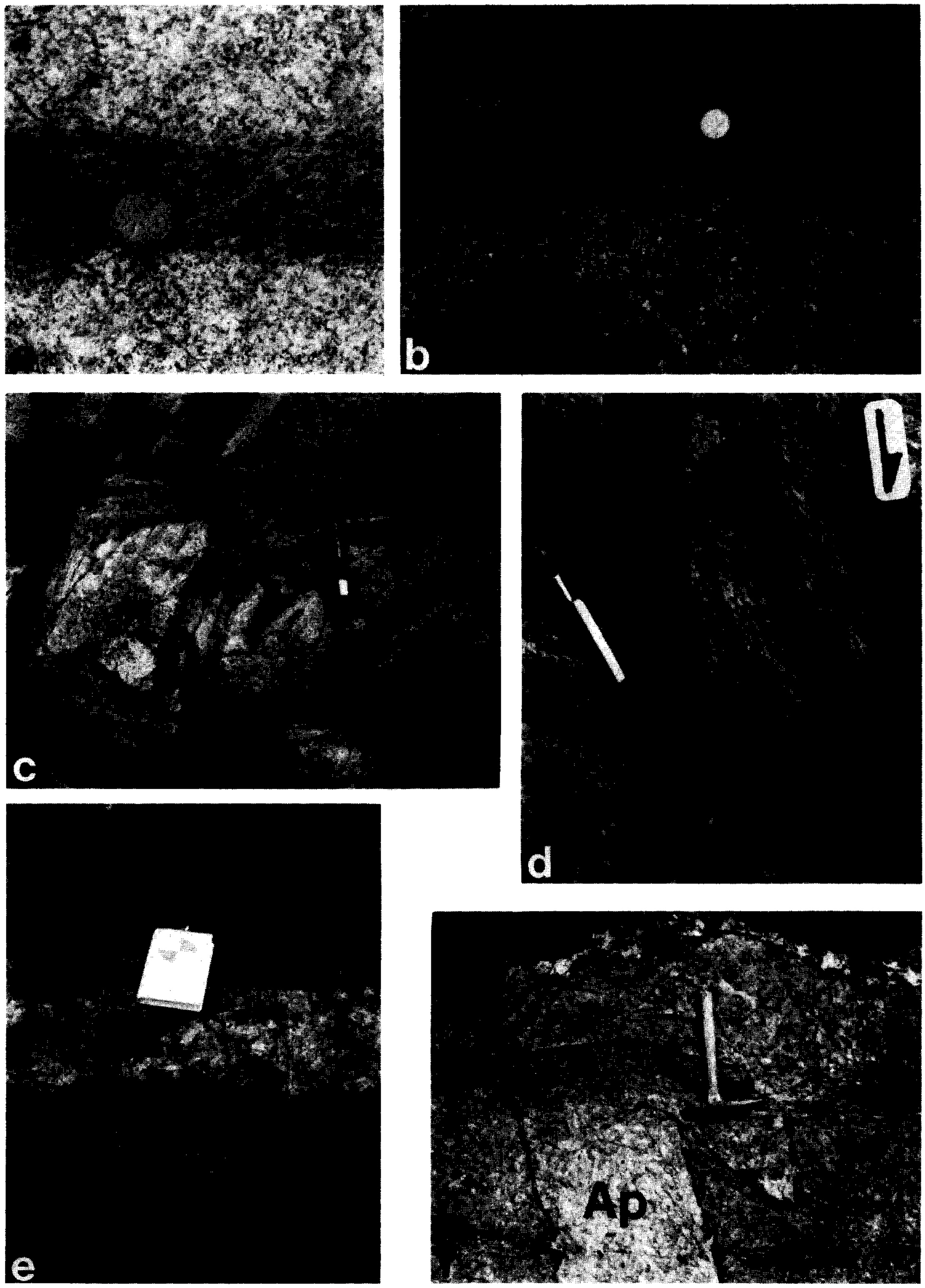

Fig. 4. Brittle/ductile shear zones of the Mooshla pluton. (a) Plan view of a continuous shear zone. Coin diameter is 2 cm. (b) Plan view of a discontinuous shear zone. Note sheared quartz veins at the shear zone boundary (szb). Coin diameter is 2 cm. (c) Field example of the anastomosing pattern displayed by the brittle/ductile shear zones. Plan view. Hammer (e.g. 30 cm-long) for scale. (d) *C/S* fabrics indicating south-directed normal-sense of shearing. Vertical section viewed towards the east. Pencil (e.g. 14 cm-long) for scale. (e) Aplite dyke crosscutting E–W trending shear zones (marked by dashed lines). Plan view. The notebook is 19 cm-long. (f) Aplite dyke (Ap) cross-cut by an E–W trending shear zone. Plan view. Hammer (e.g. 30 cm-long) for scale.

Millimetre- to centimetre-thick extensional gold- and sulphide-bearing quartz veins occur in the highly strained central parts of discontinuous shear zones. Extensional veins are essentially parallel to the boundary and/or the *C*-planes of the host shear zone, and are characterized by well-developed fiber textures. Quartz fibers are commonly oriented perpendicular to the vein walls, which is consistent with the extensional nature of the shear-related deformation. The straight aspect of quartz fibers attests to coaxial incremental extension (Ramsay and Huber, 1983). Some of the mineralized extensional veins display boudinage and pinch-and-swell structures, indicating that they were deformed by shearing following their formation. Sheared and dynamically recrystallized quartz veins parallel to the hosting shear zone boundaries occur locally, and are interpreted as extensional veins that were formed earlier during the incremental deformation history.

Joints, mineral-filled fractures and brittle faults occur in the isotropic tonalite adjacent to the anastomosing shear zones (Fig. 3). These brittle structures are subvertical and strike N–S, NW–SE or E–W; they are thus essentially parallel to the brittle/ductile shear zones and to aplite dykes cross-cutting the tonalite. As for the shear zones, most joints and fractures are characterized by cm-wide, parallel-sided and symmetrical alteration halos (Fig. 6a), which attest to extensive fluid circulation during and/or after their formation. Fractures are commonly filled by mineral assemblages mostly made up of chlorite, sericite and epidote intergrown with minor quartz, calcite and disseminated sulphides. EW-trending joints and fractures are commonly crosscut by NW-trending ductile shear zones, but EW-trending shear zones are frequently crosscut by N–S or NW–SE-trending fractures and brittle faults (Fig. 7).

Microscopic structural features

In thin section, most shear zone boundaries are gradational over less than 1 cm and are thus a sharp contact between a coarse-grained tonalite and the fine-grained mylonitic phyllonite. Figure 5(a) shows a millimetre-scale shear zone boundary that is marked by a disappearance of the mylonitic foliation in the protolith and a decrease of alteration minerals within the relatively undeformed tonalite. Close to the shear zone, the tonalite consists of 500 μm to 1 mm grains of altered plagioclase, quartz, chlorite, calcite, and sulphide minerals. Individual plagioclase crystals are more than 50% replaced by an epidote–sericite–calcite assemblage that is pervasively distributed within grains and/or concentrated along plagioclase cleavage planes and intragranular fractures. Despite the strong alteration, vestiges of magmatic zoning in plagioclase occur locally. Mafic minerals such as hornblende and biotite are replaced and pseudomorphosed by chlorite, which defines the progressive development of the mylonitic foliation at shear zone boundaries (Fig. 5a). Outside shear zones, euhedral quartz grains show undulatory extinction. Quartz recrystallization is minimal and limited to the formation of subgrains along sutured quartz boundaries. Millimetre-wide transgranular fractures are locally seen in plagioclase grains. Such fractures are filled by chlorite–epidote–sericite–quartz, and are commonly oblique to the shear zone boundaries.

Ductile deformation is accompanied by the abrupt disappearance of plagioclase (Fig. 5a) and the development of alternating chlorite – epidote $\pm$ quartz ribbons and quartz – sericite $\pm$ epidote $\pm$ chlorite ribbons. Plagioclase pseudomorphs are rarely present in areas close to shear zone boundaries but occur locally as epidote-rich porphyroblasts. The margins of shear zones typically consist of up to 15 % of quartz porphyroclasts (Fig. 5a) set in a fine-grained (< 10 μm) matrix of chorite, epidote, sericite, quartz and calcite. Quartz porphyroclasts are stretched within the foliation plane, and their long dimension can reach up to 1 cm (Fig. 5b), but porphyroclasts with long axes on the order of 500 μm or less are much more abundant. The largest quartz porphyroclasts are totally recrystallized into finer-grained crystals (Fig. 5b) that locally show well-developed individual grain-shape alignment (Ramsay and Huber, 1987) oblique to the mylonitic layering. Quartz porphyroclasts are more highly recrystallized towards the central part of the shear zones. At shear zone boundaries or close to it, quartz grains form typical σ- and δ-type porphyroclasts (Simpson and Schmidt, 1984; Hanmer and Passchier, 1991) (Fig. 5a & b), that are characterized by undulose extinction and nascent recrystallization locally associated with core-and-mantle textures (White, 1976).

Towards the central part of the brittle/ductile shear zones, S_m has been rotated into parallelism with shear zone boundaries, and the fault-related rock consists of a quartz–chlorite–epidote–sericite phyllonite in which less than 5% quartz porphyroclasts and porphyroblasts form augen in a well-foliated matrix. The mylonitic foliation is defined by alternating chlorite-rich and epidote-rich ribbons, and by the ubiquitous presence of discontinuous

Fig. 5. Photomicrographs from brittle/ductile shear zones and brittle faults of the Mooshla pluton. All photographs show a section parallel to the mineral lineation and perpendicular to the foliation (*X–Z* sections). (a) Photomicrograph illustrating a sharp boundary between the undeformed host rock and a shear zone. Note the abrupt disappearance of feldspars within the shear zone. Shear sense is dextral. Scale bar is 5 mm. (b) Recrystallized quartz porphyroclasts within a brittle/ductile shear zone. Scale bar is 5 mm. (c) Quartz ribbons and foliation-parallel extensional veinlet (arrowed in the center part of the photomicrograph) in a brittle/ductile shear zone. Note well-preserved open space filling texture in the extensional veinlet. Scale bar is 5 mm. (d) Shear bands in a brittle/ductile shear zone. Shear sense is dextral. Scale bar is 5 mm. (e) Semibrittle microcracks in quartz porphyroclasts within a shear zone. The fractures are filled by chlorite fibers. Scale bar is 1 mm. (f) Shear fractures associated with microbreccia. Ductile deformation is limited to conjuguate fractures (arrows). Scale bar is 5 mm. (g) Detail of an intergranular fracture. The fracture is filled by quartz, chlorite, carbonate and oxide minerals. Scale bar is 1 mm. (a), (f) and (g) plane light; (b), (c), (d) and (e) crossed-polars.

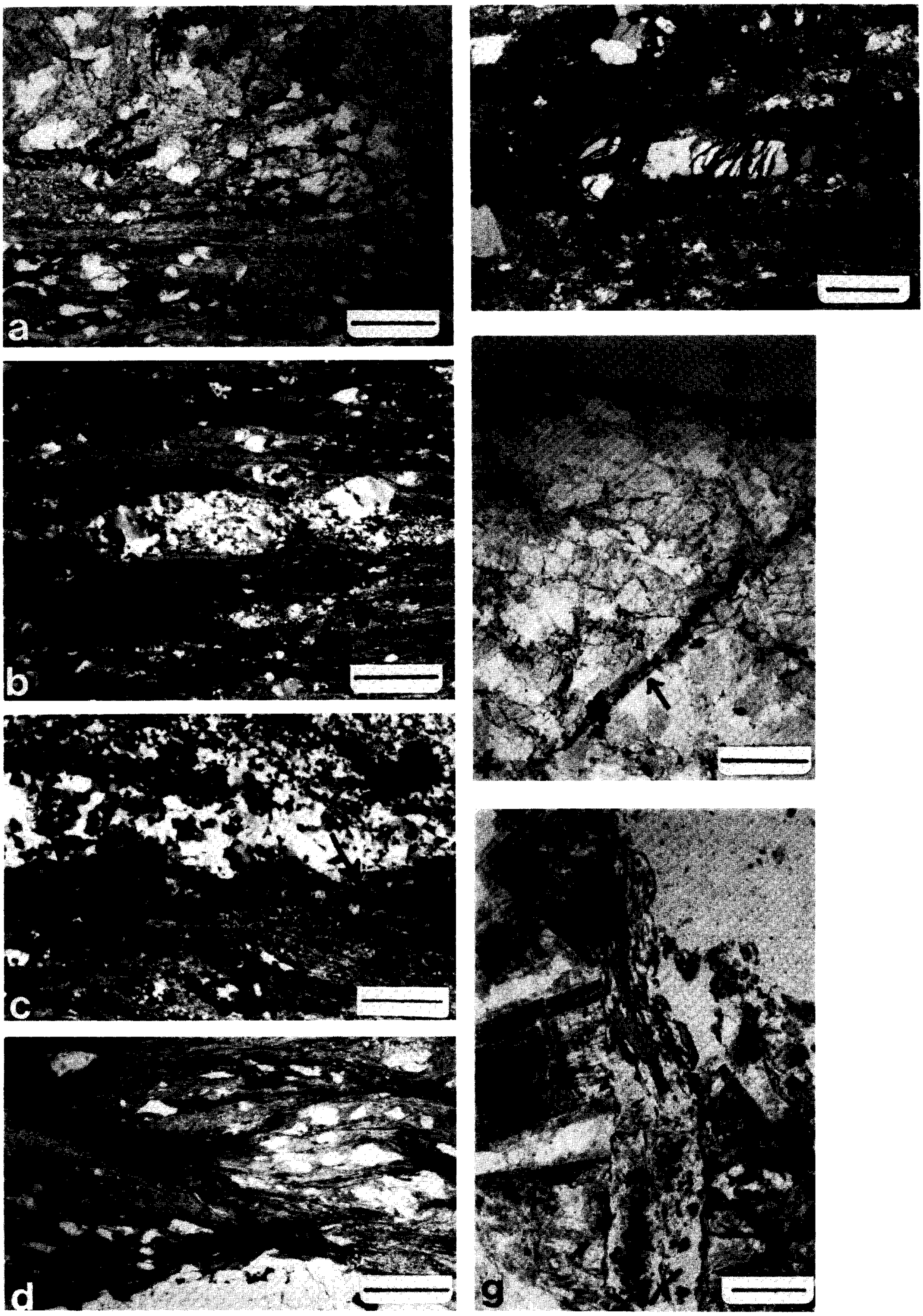
a
b
c
d
g

ribbons of fine-grained (<20 μm) recrystallized quartz grains (Fig. 5c). Such quartz ribbons originated from quartz porphyroclasts that have been strongly recrystallized and stretched as in Fig. 5b, and/or from recrystallized extensional quartz veins originally formed parallel to the mylonitic foliation as in Fig. 5c, and/or from silica produced by the breakdown of plagioclase (Williams and Dixon, 1982; Evans, 1990) and introduced in the shear zone during deformation. Sulphide neoblasts (mostly pyrite) with asymmetrical pressure fringes locally occur. *C/S* fabrics and shear bands are present (Fig. 5d). *C*-planes are commonly made up of chlorite–epidote-rich slip planes whereas *S*-planes correspond to chlorite–sericite–calcite layering and to stretched quartz porphyroclasts and porphyroblasts. Asymmetrical microfolds of the mylonitic foliation are present within the shear zones, and their vergence is consistent with other shear-sense indicators. The anastomosing character of the shear zones that is displayed at the outcrop scale (see Fig. 4c) also exists at the microscopic scale. It appears as cm-scale (and smaller) less deformed epidote – sericite – quartz ± plagioclase discontinuous domains that form relict elongate cataclastic clasts within the fine-grained matrix of the phyllonite.

Some shear zones show an array of intragranular microcracks over plastically deformed and recrystallized quartz porphyroclasts (Fig. 5e). Microscopic domains containing such fractures are commonly characterized by well-developed *C/S* fabrics in the fine-grained matrix, and are in sharp contact with domains in which *C/S* fabrics are less developed and in which quartz porphyroclasts are not fractured. The fabric is suggestive of semi-brittle cracks within individual grains as described by Mitra (1992). The intragranular cracks are not strictly brittle; they sometimes die out within individual quartz grains and never cross grain boundaries (Fig. 5e). Such intragranular fractures are frequently found in feldspar and quartz porphyroclasts within low-grade quartzofeldspathic mylonites (Mitra, 1978, 1992; FitzGerald and Stünitz, 1993). They form when there is a high proportion of fine-grained matrix; plastic flow in the matrix initiates fractures in porphyroclasts following high resolved shear stress concentrations in the porphyroclastic minerals (Mitra, 1978).

Foliation-parallel extensional quartz veinlets can be seen in thin sections (Fig. 5c). These are a few mm-wide, laterally discontinuous and locally show pinch-and-swell structures. Quartz fibers are oriented perpendicular to the veinlet walls and show a grain shape fabric typical of open-space filling (Fig. 5c). Some extensional veinlets are partly unfilled, but most are filled by an assemblage of sulphides (pyrite–hematite) and quartz. Some of these veinlets have locally preserved evidence for plastic deformation and grain-size reduction by recrystallization, which is consistent with the interpretation that such extensional veins and veinlets were formed and progressively deformed and recrystallized during the incremental development of the brittle/ductile shear zones.

Shear zone terminations and propagation features

The studied outcrop provided excellent exposures to investigate the nature of bulk strain at the ends of individual shear zones and how ductile deformation propagated. Many brittle/ductile shear zones of the Mooshla pluton terminate into undeformed surrounding rocks in which shear strain dissipated into brittle structures such as joints, mm-wide fractures and faults (Figs 6 & 7). We recognize two distinctive types of lateral terminations (i.e. terminations viewed in *Y–Z* sections, perpendicular to both the shear direction and the mylonitic foliation): Type 1 terminations, where shear zones terminate into EW- and NS-trending fractures and brittle faults (Figs 6 & 7), and Type 2 terminations, where shear zones curve progressively into adjacent brittle/ductile shear zones (Fig. 8).

Type 1 lateral terminations are more common than Type 2. Most mylonite zones narrow progressively along strike and are characterized by an overall decrease in the intensity of ductile strain. At their tips, the mylonitic fabric (foliation and *S/C* surfaces) dies out and is almost indistinguishable from the igneous fabric of the surrounding rock. Subvertical joints and entensional fractures are commonly oblique or subparallel to the shear zone boundaries (Fig. 6). Fractures are usually filled with chlorite, epidote and quartz. In the immediate vicinity of Type 1 terminations, alteration halos along joints and fractures are up to 15 cm-wide, and the widths of the halos decrease progressively towards the undeformed tonalite. Mineral fillings have locally undergone ductile deformation as indicated by widespread undulatory extinction and recrystallization textures in quartz grains. This suggests that some fractures predated the bulk ductile deformation observed in the adjacent ductile shear zones. It is also common to find EW-trending shear zones that are abruptly deflected and die out into N–S trending joints and fractures at their lateral terminations (Fig. 7), thus leading to a hypothesis of a genetic link in the development of joints, fractures and ductile shear zones. Some NS-trending fractures were activated as brittle faults that slightly displaced the brittle/ductile shear zones (Fig. 7).

Type 2 lateral terminations occur where ductile shear zones dissipate along neoformed fractures and brittle faults that progressively bend towards adjacent shear zones (Fig. 8). Lateral terminations of this type consist of curved brittle shear zone segments that resemble horsetail fractures which propagated from the tip of a brittle/ductile shear zone. In detail, numerous tiny cracks and extensional fractures occur where ductile deformation zones terminate. The fractures and joints exhibit a horsetail-like geometry at the point of maximum shear zone deflection (Fig. 8). The tip area is characterized by a transition from ductile to predominantly brittle fabrics towards the curving termination of the shear zone. This is apparent in two samples, originally separated by less than 30 cm, from a single shear zone (Figs 8c & 9); their

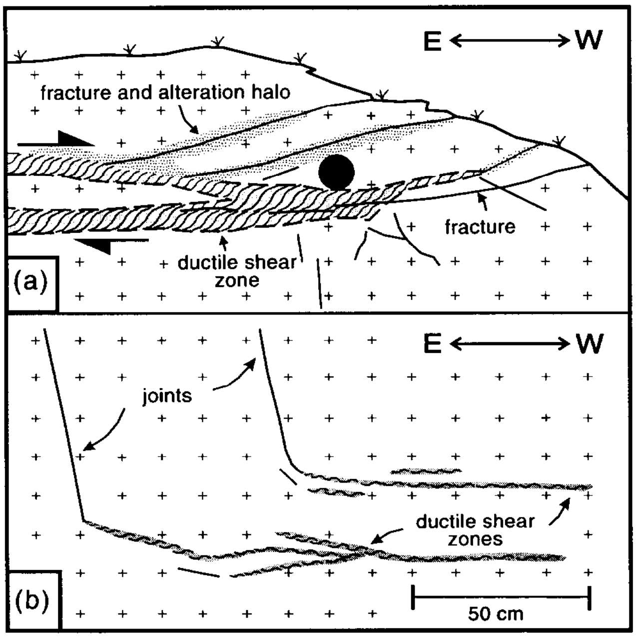

Fig. 6. (a) Field sketch showing a brittle/ductile shear zone that terminates into E–W-trending joints and fractures. Note the alteration halo associated with the brittle fractures. The lense cap (in black) is 5 cm in diameter. (b) Field sketch illustrating E–W-trending brittle/ductile shear zones that terminate into NNW–SSE trending joints. The shear zone thickness decreases progressively from west to east, it is less than 1 mm-thick at the lateral tips.

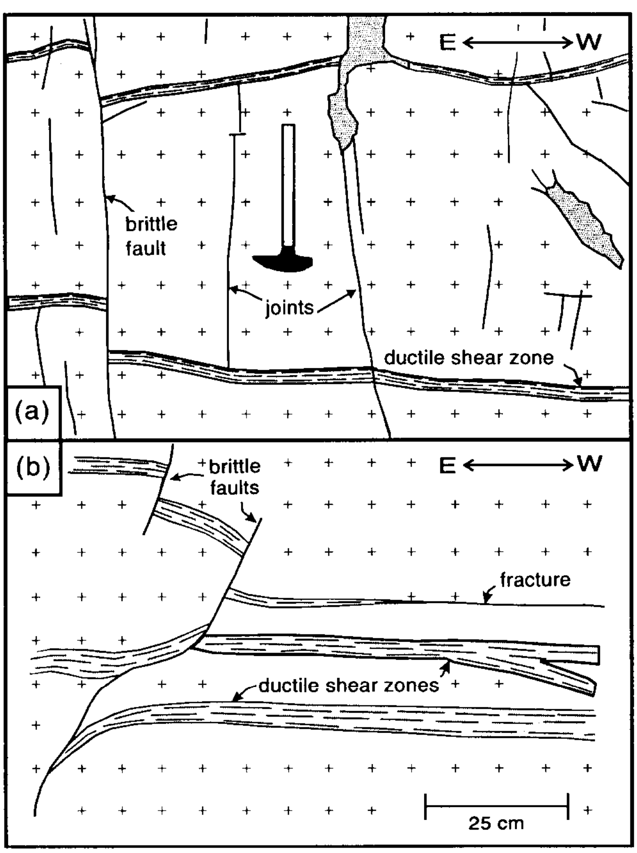

Fig. 7. Field sketches illustrating the relationships between the brittle/ductile shear zones with joints, fractures and brittle faults that cuts the surrounding tonalite. (a) E–W-trending shear zones both cross-cutting and cross-cut by joints and brittle faults. Hammer (e.g. 30 cm-long) for scale. (b) E–W-trending shear zones cross-cut by N-trending brittle faults. Note the presence of a shear zone that terminates within an E–W-trending fracture in the middle right of the field sketch.

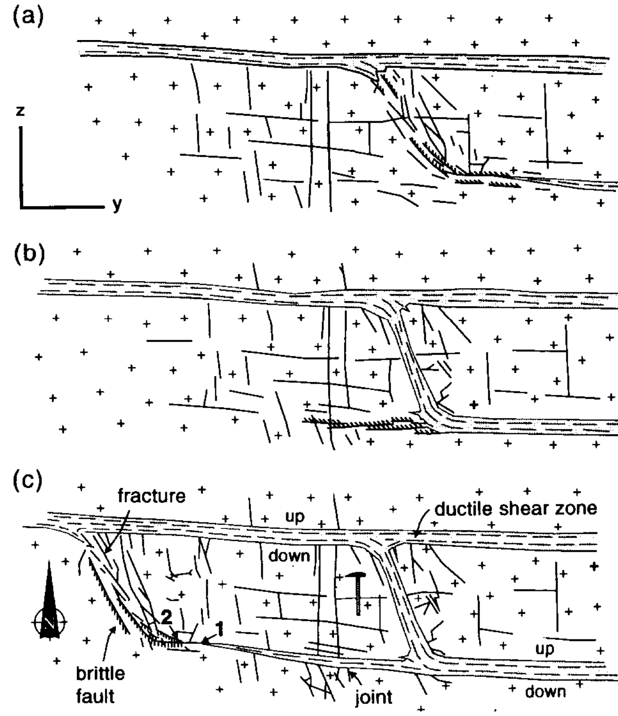

Fig. 8. Sketches illustrating the progressive development of anastomosing shear zones. (a) and (b) Ductile shear zones evolved through a stage of brittle fractures that were used as fluid conduits and propagated to form the anastomosing pattern. (c) Field example of anastomosing shear zones as they can be seen on the studied outcrop of the Mooshla pluton. Plan view perpendicular to the transport direction. Hammer (e.g. 30 cm-long) for scale. On Fig. 8(c), 1 and 2 refer to the location of samples sketched on Fig. 9(b) and (a), respectively.

structural characteristics differ significantly. Figure 9(a) shows a cm-thick ductile shear zone with structures and fabrics typical of those described above (i.e. progressive development of the foliation, porphyroclastic textures, etc.). In Fig. 9(b), ductile deformation is limited to mm-thick microfaults marked by chlorite-rich microbreccias with fragments of plagioclase and quartz (Fig. 5f). Quartz recrystallization is minimal and locally occurs along chlorite-rich ductile microshears and associated fractures. Fractures and microfaults are homogenously distributed between the microshears (Fig. 9b) and consist of extensional fractures oriented parallel to the microshear boundaries, and of high-angle fractures that are antithetic to the microshears. The latter fractures are intergranular (Fig. 5g) and filled with chlorite–quartz–sericite cataclastic breccias. Structures and fabrics of this sample indicate the predominance of cataclasis rather than plastic deformation.

DISCUSSION

Lateral terminations features described above for normal-sense shear zones of the Mooshla pluton are similar to those of strike-slip ductile shear zones as depicted by Simpson (1983). However, lateral terminations of strike-slip faults correspond to Mode II (sliding;

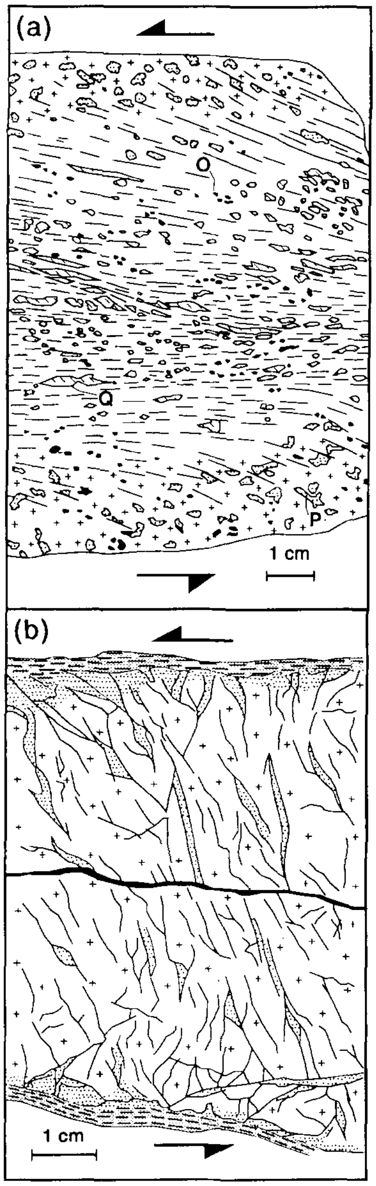

Fig. 9. Thin section sketches of end-members fabrics found along a single shear zone termination. See Fig. 8(c) for location. (a) Sketch illustrating the ductile segment of the shear zone. Textures of this sample are similar to photomicrograph in Fig. 5(a). Dotted minerals are plagioclase (P), black dots are opaque minerals (O), and white minerals are quartz grains (Q). Dashed lines represent the trace of the mylonitic foliation. (b) Sketch illustrating conjugate shear fractures associated with small-scale ductile shears in the brittle segment of the shear zone termination. Dashed lines are for ductile deformation. Dots are for brecciated material and/or quartz–chlorite open-space fillings. Black lines are for fractures. The thick black line in the middle of the sketch represent a neoformed fracture due to sample preparation.

i.e. exposed in X–Z sections) damage zone fault tips of McGrath and Davison (1995), whereas lateral terminations of dip-slip shear zones, as exposed in the Mooshla pluton, correspond to their Mode III (tear) fault tips (i.e. exposed in Y–Z sections). For strike-slip shear zones in granitic rocks, Simpson (1983) described two types of lateral terminations and argued that both formed under non-plane strain conditions of deformation. Ingles (1986) has shown, however, that these two types of terminations represent two successive stages of the same process and were formed under plane strain conditions. For type II terminations of Simpson (1983) (which are similar to Type 1 terminations described above), it was argued that splay faults and fractures formed along shear zones with relatively high shear strain and where there is a steep gradient to zero displacement at the tip of the main fault. However, Simpson (1983) suggested that a steep gradient along splays can be associated with pre-existing extension fractures, and that the relative timing of the ductile and brittle modes of failure is critical for interpreting that type of shear zone termination. In the Mooshla pluton, field observations indicate that the formation of joints and other brittle fractures occurred both before and after the bulk ductile deformation that led to the formation of phyllonites. Relationships exposed at the tip of some ductile shear zones indicate that pre-existing fractures were used as compensatory structures, thus leading to the formation of terminations similar to those described by Simpson (1983).

The Type 2 shear zone termination of the studied outcrop is typical of Mode II terminations of McGrath and Davison (1995), which have been attributed to plane strain conditions by Ramsay (1980). Horsetail fractures at the fault tip can be attributed to their progressive rotation towards the maximum principal stress (σ_1) (McGrath and Davison, 1995). In the Mooshla pluton, such fracture patterns led to the formation of anastomosing shear zones (Fig. 8; see also Fig. 4c). Our interpretation of the anastomosing brittle/ductile shear zones (Fig. 8) is that the cataclasite of Fig. 9(b) records an earlier deformational stage that led to the formation of a mylonitic phyllonite as in Fig. 9(a). Such relationships suggest that the propagation of brittle/ductile shear zones evolved through a stage of cataclastic deformation characterized by narrow fractures linked one to another. These transgranular fractures anastomosed, widened the fault zone, and incorporated wallrock fragments that continue to fracture and undergo grain-size reduction. The fractures were subsequently used as easy-slip surfaces for initial displacement and for the lateral growth of propagating brittle/ductile shear zones.

For plane strain conditions of deformation, Ramsay and Allison (1979) argued that the displacements at the shear zone tips must die out over a gradually wider area into undeformed rocks. In such a case, the lateral tip of dextral strike-slip shear zones commonly curves in a clockwise sense, and in an anticlockwise sense for sinistral shear zones (Ramsay, 1980). The incremental evolution of overlapping shear zones under plane strain deformation will thus lead to the development of an anastomosing pattern of shear zones in the X–Z plane of finite deformation. Type 2 lateral terminations described above for the Mooshla pluton show curvature features that are consistent with normal-sense shearing under plane strain conditions as the deformation area progressively widens away from shear zone tips (Fig. 8c). For layered rocks, however, McGrath and Davison (1995) found that damage zones at fault tips are different for

Mode II and Mode III edges of normal faults. Mode II edges are characterized by horsetail fractures, whereas isolated en echelon fractures unlinked to fault tips are characteristic of Mode III edges. This has been attributed either to a different mode of fracture propagation at the dip-slip and lateral edges of normal faults, or to the difference in the orientation of layering in relation to the propagation direction of fault tips (McGrath and Davison, 1995). The geometry of the lateral terminations of some brittle/ductile shear zones of the Mooshla pluton indicate that, in isotropic rocks such as granites, horsetail fractures also occur along Mode III edges of normal-sense shear zones, and that geometrical differences between Mode II and Mode III edges of normal faults (as described by McGrath and Davison, 1995) are most probably due to pre-existing layering in anisotropic rocks.

SHEAR ZONE DEVELOPMENT AND EVOLUTION IN THE MOOSHLA PLUTON

There are critical observations and/or structural relationships that one should consider before any attempt can be made to propose a sequential model of evolution for brittle/ductile shear zones of the Mooshla pluton.

(1) The spatial association of joints, fractures, brittle faults and brittle/ductile shear zones in the Mooshla pluton, their gradational relationships and identical orientations, and the similarity of their mineral fillings indicate that they are genetically related and formed under similar stress states and metamorphic grade. Similar relationships between joints and shear zones have been described by Segall and Pollard (1983), and Segall and Simpson (1986) noted such a relationship for ductile shear zones that nucleated and terminated on dilatant fractures. The fact that joints, fractures and faults of similar orientations both crosscut and are crosscut by the shear zones indicates that brittle fracturing both preceded and succeeded the bulk of the incremental ductile deformation.

(2) The relations of brittle/ductile shear zone terminations with cataclastic fractures and microbreccias suggest that the onset of localized ductile shearing in the Mooshla pluton followed an initial stage of fluid-assisted cataclasis and related alteration of wallrocks. The spatial association of fractures with chloritic and sericitic alteration implies that fluids interacted with the wallrock and participated in mineral reactions.

(3) The presence of alteration halos along joints, fractures and shear zones, and the occurrence of quartz veins in the brittle/ductile shear zones indicates that a significant volume of fluid was present during both brittle fracturing and ductile shearing. The nature of alteration minerals suggests that fluid circulation led to the pervasive transformation of plagioclase and Fe–Mg-bearing minerals (biotite, hornblende) into softer phyllosilicate-rich assemblages. Plagioclase, hornblende and biotite occur in greatest abundance in the least deformed tonalite, and are absent in the mylonitic material. The decreasing content of these minerals with deformation is accompanied by a marked increase in epidote–sericite and chlorite, and it is extremely likely that epidote–sericite and chlorite are developing at the expense of plagioclase, hornblende and biotite. In terms of mineralogy, the overall effect of deformation has been to change an assemblage consisting dominantly of quartz and plagioclase to one consisting dominantly of quartz, epidote–sericite and chlorite. A consistent corollary is that the predominant softening mechanism that allowed strain localization was reaction softening (White and Knipe, 1978).

Based on the presence of mutual crosscutting relations between the 2702 $\pm$ 4 Ma aplite dykes (Tremblay *et al.*, 1995) and brittle/ductile shear zones of the Mooshla pluton, and on evidence for the coeval development of shear zones and associated alteration, the age of aplite dykes is interpreted as an accurate estimate for the timing of ductile deformation. Such timing is similar, within error, to the age of surrounding volcanic rocks of the Blake River Group. This suggests that fluids which have been drained into the brittle/ductile shear zones during deformation originated from hydrothermal activity during, or immediately after the latest stage of volcanism and associated plutonism at ca 2702 $\pm$ 4 Ma.

Successive stages in the evolution of brittle fractures and brittle/ductile shear zones of the Mooshla pluton are illustrated on Fig. 10. Subvertical joints and fractures were the first structures to form in the pluton. Fractures

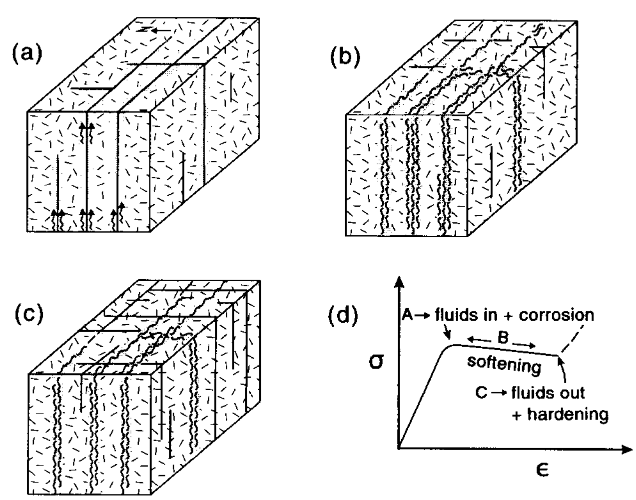

Fig. 10. Sketches illustrating an evolutionary model and the interpretation of brittle/ductile shear zones of the Mooshla pluton. (a) Brittle fractures first formed and were used as fluid conduits for the alteration and the weakening of the granitic material. (b) Ductile shear zones developed along pre-existing fractures and joints by reaction softening of host rocks. (c) Deformation regime went back to brittle conditions (by decreasing fluid input) and joints and fractures cross-cutting the brittle/ductile shear zones were formed. (d) Stress–strain diagram illustrating the evolution of deformation from a to c.

probably developed through extension due to hydraulic fracturing in conditions of high fluid pressure and low differential stress (Secor, 1965; Pollard and Aydin, 1988). These initial fractures played a significant role in both allowing fluid circulation and wallrock alteration, and subsequently localizing ductile deformation. Each stage of grain fracturing created new surface area on which chemical reactions can start to produce a more ductile matrix. This occurred under greenschist grade metamorphic conditions as indicated by chlorite–epidote–sericite–quartz fillings found within most fractures. Fluid circulation was promoted by hydraulic gradients (Sibson, 1981), and the opening of dilatant fractures produced local zones of low fluid pressure acting as fluid-activated valves that promoted extensive fluid infiltration and circulation (Fig. 10a). Brittle fracturing also enhanced permeability by grain-scale dilatancy toward the opening of boundary voids and cleavage cracks in minerals such as feldspars and amphiboles. We speculate that fractures propagated by subcritical crack growth in conditions of stress corrosion are enhanced by the presence of hydrothermal fluid at supralithostatic pressure.

The pervasive mineral alteration along joints and fractures weakened the tonalitic protolith and promoted shear strain localization under an overall constant bulk stress field (Fig. 10b). The development of foliation-parallel quartz veins within brittle/ductile shear zones reflects an increase in fluid pressure during the incremental ductile deformation. These quartz veins and veinlets belong to types A and B of McCaig (1987) with extension directions essentially perpendicular or slightly oblique to the vein boundaries. The formation of such extensional veins does not require wallrock deformation and is compatible with simple shear deformation mechanisms (see Ramsay and Graham, 1970).

As ductile deformation became predominant, shear zones began to grow in length and in width. Cobbold (1977) suggested that width variations of shear zones can be attributed to alternating strain-softening and strain-hardening mechanisms during progressive simple shear. In the Mooshla pluton, the widening of ductile shear zones has been mainly controlled by the volume (thickness) of rocks that were sufficiently fractured and altered prior to, and during ductile deformation. These shear zones were not initiated as ductile shear zones. We believe that they formed when reaction-softening, brittle fracturing and microbrecciation reached a critical point. Evidence for such an evolution is locally preserved at the lateral termination of some brittle/ductile shear zones, as shown in Fig. 8 where brittle and ductile fabrics are found along the same structure. A similar deformation scenario has been described by Gibson (1990) for the nucleation and growth of retrograde shear zones in foliated rocks.

We suggest that with decreasing fluid input into the shear zone, the bulk of the ductile deformation regime gave way to brittle conditions under the same stress field, which led to the formation of joints and fractures crosscutting the shear zones (Fig. 10c). These crosscutting fractures were probably formed during an advanced stage of shear deformation when steady state ductile deformation progressively vanished. These fractures show the same mineralogy as the earlier ones but are commonly devoid of altered wallrocks at their margins.

A hypothetical strain–stress curve is shown in Fig. 10(d). The deformational path from the origin towards point A represents the early stage of fluid-assisted fracturing and corresponds to the formation of early joints and fractures (Fig. 10a). This part of the curve indicates that stress had to increase in order to cause brittle fracturing in the pluton. Fluids promoted extensive wall-rock alteration and the chemical transformation of primary minerals into softer ones, and assisted fracture development until a point at which the protolith was sufficiently softened that it deformed by ductile mechanisms within steady-state (and even decreasing) stress conditions (path B on Fig. 10d). At the end of one (or several) stage(s) of fluid production and pumping into deformation zones, strain–stress relationships went back to dryer (hardening) conditions until a point (point C on Fig. 10d) where stress had to increase in order to get brittle fracturing of the pluton and of its already sealed shear zones.

CONCLUSION

The initiation, growth and terminations of brittle/ductile shear zones crosscutting the Mooshla pluton are the result of alternating stages of brittle and ductile deformation. Our observations suggest that ductile deformation that led to the formation of mylonitic phyllonites was preceded and succeeded by short-lived brittle strain increments, which are associated with the formation of joints and fractures that both crosscut and are crosscut by the phyllonites. Metre-scale brittle/ductile shear zones initiated along previously formed fractures and played a fundamental role in both allowing fluid infiltration and circulation, and localizing ductile deformation. The initial fractures were filled by hydrothermal minerals (chlorite, epidote, sericite, quartz, calcite). The synchronous alteration of wallrocks promoted softening processes such as reaction-enhanced ductility and hydraulic weakening. As fractures became long enough to mechanically interact, shear strain concentration was facilitated and promoted the propagation of incipient shear zones. The concomitant and cyclic influx of fluids was accompanied by increasing metasomatic reactions that led to increased softening in the shear zones.

Acknowledgements—The authors would like to acknowledge Daniel Patry for helpful collaboration during the mapping of the studied outcrop. Thanks are due to Paul Sacks for the reviewing of an earlier version of the manuscript and to Barbara Fortin and Yvon Houde for drawing the figures. Formal reviews by L. Pryer, G. Mitra and S. F. Wojtal improved the manuscript. The National Research Council of

Canada (NSERC: OGP-105669) and the Fonds pour la Formation de Chercheurs et l'Aide à la Recherche (FCAR: grant 95-ER-2270) subsidized this contribution as operating grants to A. Tremblay. This is contribution 96-5130-05 of the *Ministère des Ressources Naturelles, Québec*.

REFERENCES

Bell, T. H. and Hammond, R. L. (1984) On the internal geometry of mylonite zones. *Journal of Geology* **92**, 667–686.

Boyer, S. E. and Elliott, D. (1982) Thrust systems. *Bulletin American Association Petroleum Geology* **66**, 1196–1230.

Burg, J. P. and Laurent, Ph. (1978) Strain analysis of a shear zone in a granodiorite. *Tectonophysics* **47**, 14–42.

Bürgmann, R. and Pollard, D. D. (1994) Strain accommodation about strike-slip fault discontinuities in granitic rock under brittle-to-ductile conditions. *Journal of Structural Geology* **16**, 1655–1674.

Cobbold, P. R. (1977) Description and origin of banded deformation structures, II, Rheology and the growth of banded perturbations. *Canadian Journal of Earth Sciences* **14**, 2510–2523.

Corfu, F., Krogh, T. E., Kwok, Y. Y. and Jensen, L. S. (1989) U–Pb zircon geochronology in the southwestern Abitibi greenstone belt Superior province. *Canadian Journal of Earth Science* **26**, 1747–1763.

Coward, M. P. (1976) Strain within ductile shear zones. *Tectonophysics* **34**, 181–197.

Coward, M. P. and Potts, G. J. (1983) Complex strain patterns developed at the frontal and lateral tips to shear zones and thrust zones. *Journal of Structural Geology* **5**, 383–399.

Dimroth, E., Imreh, L., Goulet, N. and Rocheleau, M. (1983) Evolution of the south-central segment of the Archean Abitibi Belt, Quebec, Part III: plutonic and metamorphic evolution and geotectonic model. *Canadian Journal of Earth Sciences* **20**, 1374–1388.

Evans, J. P. (1990) Textures, deformation mechanisms, and the role of fluids in the cataclastic deformation of granitic rocks. In: *Deformation Mechanisms, Rheology and Tectonics*, eds R. J. Knipe and E. H. Rutter, Vol. 54, pp. 29–39 Special Publication of Geological Society, London.

FitzGerald, J. D. and Stünitz, H. (1993) Deformation of granitoids at low metamorphic grade I: Reactions and grain size reduction. *Tectonophysics* **221**, 269–297.

Gaudreau, R. (1986) Intrusion synvolcanique et minéralisations aurifères: exemple du pluton de Mooshla, canton de Bousquet, Abitibi, Unpublished M.Sc. thesis, University of Laval.

Gibson, R. G. (1990) Nucleation and growth of retrograde shear zones: an example from the Needle Mountains Colorado, U.S.A. *Journal of Structural Geology* **12**, 339–350.

Hanmer, S. and Passchier, C. (1991) Shear-sense indicators: a review, *Geological Survey of Canada Paper*, **90-17**.

Ingles, J. (1986) Terminations of ductile shear zones. *Tectonophysics* **127**, 87–95.

Langshur, A. (1991) The geology, geochemistry and structure of the Mooshla intrusion, Bousquet mining center, Quebec, Unpublished M.Sc. thesis, Ottawa University.

Losh, S. (1989) Fluid–rock interaction in an evolving ductile shear zone and across the brittle–ductile transition Central Pyrenees, France. *American Journal of Science* **289**, 600–648.

Ludden, J., Hubert, C. and Gariépy, C. (1986) The tectonic evolution of the Abitibi greenstone belt of Canada. *Geological Magazine* **123**, 153–166.

McCaig, A. M. (1987) Deformation and fluid–rock interaction in metasomatic dilatant shear bands. *Tectonophysics* **135**, 121–132.

McGrath, A. G. and Davison, I. (1995) Damage zone geometry around fault tips. *Journal of Structural Geology* **17**, 1011–1024.

Mitra, G. (1978) Ductile deformation zones and mylonites: the mechanical processes involved in the deformation of crystalline basement rocks. *American Journal of Science* **278**, 1057–1084.

Mitra, G. (1992) Deformation of granitic basement rocks along fault zones at shallow to intermediate crustal levels. In: *Structural Geology of Fold and Thrust Belts*, eds S. Mitra and G. W. Fisher, pp. 123–144, The Johns Hopkins University Press, Baltimore.

Mortensen, J. K. (1993) U–Pb geochronology of the eastern Abitibi subprovince. Part 2: Noranda–Kirkland Lake area. *Canadian Journal of Earth Science* **30**, 29–41.

Newman, J. and Mitra, G. (1993) Lateral variations in mylonite zone thickness as influenced by fluid–rock interactions, Linville Falls fault North Carolina. *Journal of Structural Geology* **15**, 849–863.

O'Hara, K. (1988) Fluid flow and volume loss during mylonitization: an origin for phyllonite in an overthrust setting North Carolina, U.S.A. *Tectonophysics* **156**, 21–36.

Pollard, D. D. and Aydin, A. (1988) Progress in understanding jointing over the past century. *Bulletin of Geological Society America* **100**, 1181–1204.

Ramsay, J. G. (1980) Shear zone geometry: a review. *Journal of Structural Geology* **2**, 83–89.

Ramsay, J. G. and Allison, I. (1979) Structural analysis of shear zones in an alpinized Hercynian granite. *Schweizerische mineralogische und petrographische Mitteilurgen* **59**, 251–279.

Ramsay, J. G. and Graham, R. H. (1970) Strain variations in shear belts. *Canadian Journal of Earth Science* **7**, 786–813.

Robert, F. (1989) Internal structure of the Cadillac tectonic zone southeast of Val d'Or, Abitibi greenstone belt, Quebec. *Canadian Journal of Earth Science* **26**, 2661–2675.

Secor, D. T. (1965) Role of fluid pressure in jointing. *American Journal of Science* **263**, 633–646.

Segall, P. and Pollard, D. D. (1983) Nucleation and growth of strike slip faults in granite. *Journal of Geophysical Research* **88**, 555–568.

Segall, P. and Simpson, C. (1986) Nucleation of ductile shear zones on dilatant fractures. *Geology* **14**, 56–59.

Sibson, R. H. (1981) Fluid flow accompanying faulting: field evidence and models, In: *Earthquake prediction: an international review*, eds D. W. Simpson and P. G. Richards, Vol. 4, pp. 593–603, American geophysics Union, Maurice Ewing Ser.

Simpson, C. (1983) Displacement and strain patterns from naturally occurring shear zone terminations. *Journal of Structural Geology* **5**, 497–506.

Simpson, C. (1985) Deformation of granitic rocks across the brittle–ductile transition. *Journal of Structural Geology* **7**, 503–511.

Simpson, C. and Schmidt, S. M. (1984) An evaluation of criteria to deduce the sense of movement in sheared rocks. *Bulletin of Geological Society America* **94**, 1281–1288.

Stone, W. E. (1990) Archean volcanism and sedimentation in the Bousquet gold district, Abitibi greenstone belt, Québec: implications for stratigraphy and gold concentration. *Bulletin of Geological Society America* **102**, 147–158.

Stünitz, H. and FitzGerald, J. D. (1993) Deformation of granitoids at low metamorphic grades II: Granular flow in albite-rich mylonites. *Tectonophysics* **221**, 299–324.

Takagi, H. (1989) Ductile shear zones: microstructures of mylonites, In: *Rheology of Solids and of the Earth*, eds. S. I. Karato and M. Toriumi, Oxford University Press, Oxford.

Tourigny, G. (1991) Archean volcanism and sedimentation in the Bousquet gold district, Abitibi greenstone belt, Quebec: implications for stratigraphy and gold concentration: alternative interpretation and reply. *Bulletin of Geological Society America* **103**, 1253–1257.

Tourigny, G. and Chartrand, F. (1994) Kinematic evolution of metrescale shear zones in foliated low-grade tectonites: an example from the Bousquet gold district Quebec. *Canadian Journal of Earth Science* **31**, 1301–1308.

Tremblay, A., Tourigny, G. and Machado, N. (1995) Zircon U/Pb age constraints on deformation and gold mineralization of the Mooshla pluton, southern Abitibi Belt, Canada, *Geological Society America Abstracts with Programs*, **27/6**, A-163.

Vauchez, A. (1987) The development of discrete shear-zones in a granite: stress, strain and changes in deformation mechanisms. *Tectonophysics* **133**, 137–156.

White, S. H. (1976) The effects of strain on microstructures, fabrics and deformation mechanisms in quartzites. *Philosopical Transactions Society, London*, Series **A283**, 69–86.

White, S. H. and Knipe, R. J. (1978) Transformation- and reaction-enhanced ductility in rocks. *Journal of Geological Society London* **135**, 513–516.

White, S. H., Burrows, S. E., Carreras, J., Shaw, N. D. and Humphrey, F. J. (1980) On mylonites in ductile shear zones. *Journal of Structural Geology* **2**, 175–187.

Williams, G. and Dixon, J. (1982) Reaction and geometrical softening in granitoid mylonites. *Text. and Microstr.* **4**, 223–239.